PHYSICAL REVIEW B **66**, 161401(R) (2002)

Bend-induced insulating gap in carbon nanotubes

L. F. Chibotaru, S. A. Bovin, and A. Ceulemans
Department of Chemistry, University of Leuven, Celestijnenlaan 200F, B-3001 Leuven, Belgium
(Received 29 July 2002; published 1 October 2002)

The effect of uniform bend on the electronic structure of single wall carbon nanotubes is investigated as function of diameter, chirality, and plane of bend. This deformation can only mix states with the same projection of **k** on the tube's axis and belonging either to one nanotube line or to nearest neighbor and next nearest neighbor lines. The bend-induced insulating gap opens in chiral and zigzag tubes, scales as the square of the bend curvature and is strongly dependent on the chirality of the tube. For large diameters of the tubes, the bend-induced gap scales as the square of the tube's diameter and is strongly determined by the changes of the bond lengths. The observation of these gaps should become possible with current experimental techniques.

DOI: 10.1103/PhysRevB.66.161401 PACS number(s): 72.80.Rj, 73.61.Wp, 85.65.+h

Since their discovery,[1] carbon nanotubes attracted much attention, first of all as molecular conductors.[2] Close to the Fermi level the electronic structure of single wall nanotubes (SWNT's) corresponds to the folding of the graphene π bands to equidistant lines of allowed **k** states on the graphene's Brillouin zone.[3–6] Straight SWNT's can be either metallic or semiconducting depending on their chirality.[3–5] Metallicity is associated with the crossing of the graphene's Fermi points K_1 and K_2 by the nanotube's lines. Such an intersection takes place in tubes, called primary metallic, for which the difference of the nanotubes indices, n and m [integers defining the chiral vector of the SWNT (Ref. 7)], is divisible by 3. Other tubes, called primary semiconducting, display an insulating gap proportional to the distance from the $K_1(K_2)$ point to the closest nanotube line. This gap scales as $1/R_t$ with the radius R_t of the tube of a given chirality. The curvature of the nanotube's surface leads to different transfer parameters for pairs of carbon atoms having different orientations relative to the tube's axis. This results in the opening of a gap at the Fermi level in all primary metallic SWNT's, roughly scaling as $1/R_t^2$, except for the armchair $(m=n)$ tubes which remain metallic.[5,8]

Structural deformations seem to be common to SWNT materials and devices. Two kinds of deformations have been observed: local and distributed over the length of the tube. Strong local bend strains result in kinks,[9–11] the main modifications of the electronic structure being associated with local $\sigma-\pi$ hybridization.[12,13] It was shown that localized states arise in the region of bend leading to the decrease of the transmission at the Fermi level.[12,14] Distributed band deformations, uniform bends, are the main structural distortions in coiled and toroidal SWNT's.[15–17] A common feature of all uniformly distributed deformations is that they do not lead to significant $\sigma-\pi$ hybridization.[8,12] At the same time the uniform bend essentially differs from other uniform deformations (twist, radial, and axial stretch/compression). Deformations of the latter kind can only induce homogeneous distortions of the graphene strip from which the nanotube is rolled up while preserving in full the translational symmetry of the corresponding graphene lattice. This allowed for simple analytical treatments of the effect of these strains on the π bands of the tubes.[8,18,19] By contrast the uniform bend of the SWNT removes the original translational symmetry of the corresponding graphene strip, and complicates much both analytical and numerical treatments of the problem. As a consequence, the effect of a uniform bend was considered till now only for armchair nanotubes within a continuous model describing the electronic states close to K_1 and K_2 in a long wavelength approximation.[8] It was found that the gap does not open in these tubes, which is a pure symmetry effect.[8] At the same time no mechanism for the gap opening and estimation of the effect in different tubes is available. It is therefore most important to predict the effects of these deformations on the electronic structure of different tubes in order to assess their behavior as molecular wires. In the present paper we fill in this gap by analytically investigating the bend-induced insulating properties of SWNT's as function of their radius, chirality, and plane of bend.

In the Hückel tight-binding model, widely used in π band structure calculations of the nanotubes,[7] the interaction of the electronic states with structural deformations comes from the change of the $\pi\pi$ transfer parameters for nearest neighbor carbon atoms. Both the misalignment of the π orbitals on the neighbor carbon atoms[8,19] and the change of the bond lengths[8,18] were previously considered as the main effect of the distortion on the transfer parameters. While in straight nanotubes the effect of the bond length change was sometimes neglected, the uniform bend of the tubes with unchanged interatomic distances is not possible for geometrical reasons. We consider therefore the general form of the transfer parameter between arbitrarily oriented π orbitals on the atoms i and j by using the Slater-Koster scheme,[20]

$$\gamma_{ij}=V_{pp\pi}(r_{ij})\mathbf{n}_{1\perp}\cdot\mathbf{n}_{2\perp}+V_{pp\sigma}(r_{ij})n_{1\parallel}n_{2\parallel}, \qquad (1)$$

with resonance integrals dependent on the interatomic distance r_{ij}. In this equation, $\mathbf{n}_{i\perp}$ and $n_{i\parallel}$ are the projections of a unit vector, normal to the surface of the tube at the position of atom i, respectively on the plane perpendicular to and on the axis parallel to the bond vector $\mathbf{r}_{ij}$. To simplify further treatment, we express γ_{ij} through one single resonance integral $V_{pp\pi}(r_{ij})$, by inserting into Eq. (1) the relation $V_{pp\sigma}(r_{ij})=-\kappa V_{pp\pi}(r_{ij})$, where κ is a positive constant.

The positions of the carbon atoms on the surface of a uniformly bent tube are described by two angles, θ and φ, as specified in Fig. 1(a). The shift in the bend's angle for a

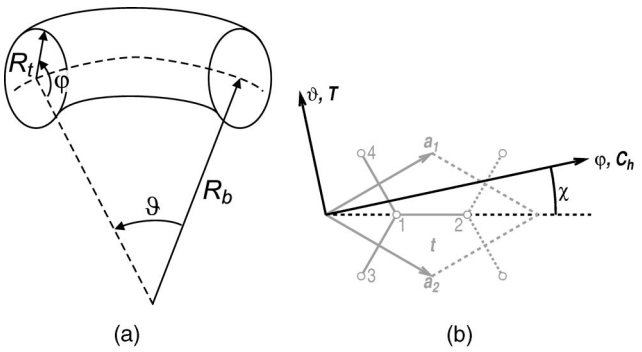

FIG. 1. (a) Angular coordinates system of a uniformly bend SWNT with radius of bend R_b. (b) The orientation of the graphene's unit cell $\boldsymbol{t}$ (containing the carbon atoms 1 and 2) relative to the chiral ($\boldsymbol{C}_h$) and the tube's axis ($\boldsymbol{T}$) vectors, defining the axes of the ϑ,φ coordinate system, for a nanotube of chirality χ. The solid lines connecting atom 1 to its nearest neighbors denote the bonds for three nonequivalent pairs.

given pair ij of carbon atoms, $\Delta\theta_{ij}=\theta_i-\theta_j$, is proportional to the curvature of the bend, $1/R_b$:

$$\Delta\theta_{ij}=\sin(\chi_{ij})\Delta\theta,$$

$$\Delta\theta=r_{CC}/R_b, \tag{2}$$

where r_{CC} is the carbon-carbon distance in graphene and χ_{ij} is the angle between the corresponding bond in the graphene plane and the chiral vector $\mathbf{C}_h$; it can be easily expressed through the chiral angle χ of the nanotube [Fig. 1(b)]. For a small curvature of the bend the transfer parameter γ_{ij} can be expanded in lower powers of $\Delta\theta$,

$$\gamma_{ij}=\gamma_{ij}^{(0)}+\gamma_{ij}^{(1)}\Delta\theta+\frac{1}{2}\gamma_{ij}^{(2)}\Delta\theta^2, \tag{3}$$

where the zeroth-order term is the transfer parameter for a straight SWNT. As it follows from Eq. (2), the restriction to the second order after $\Delta\theta$ is justified whenever $r_{CC}\ll R_b$, i.e., in all cases of practical interest. Applying this expansion to the general form in Eq. (1) one obtains the following dependence of the expansion coefficients in Eq. (3) on the circumferential positions of the two carbon atoms,[21]

$$\gamma_{ij}^{(1)}=c_{ij}^{(1)}(\cos\varphi_i+\cos\varphi_j),$$

$$\gamma_{ij}^{(2)}=c_{ij}^{(2)}(\cos^2\varphi_i+\cos^2\varphi_j)+c_{ij}^{(3)}\cos\varphi_i\cos\varphi_j, \tag{4}$$

where the coefficients c_{ij} are linear in $V_{pp\pi}(r_{CC})$ and $\partial V_{pp\pi}(r_{CC})/\partial r$ and only depend on the angle χ_{ij}. Therefore there are only three different coefficients c_{ij} associated with three nonequivalent pairs of carbon atoms shown in Fig. 1(b). By contrast, the φ_i coordinates depend on the positions of the corresponding carbon atoms in the graphene's strip, and should be actually understood as $\varphi_i^{\mathbf{t}}$,

$$\varphi_i^{\mathbf{t}}=\varphi_{\mathbf{t}}+\delta\varphi_i, \tag{5}$$

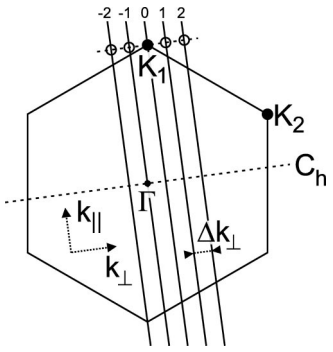

FIG. 2. Part of folded Brillouin zone of graphene corresponding to a primary metallic nanotube (straight solid lines), showing the states (open circles) which can interact with the states from the K_1 point when the tube is subjected to a uniform bend.

where $\varphi_{\mathbf{t}}$ is the φ coordinate of the unit cell $\mathbf{t}$, and $\delta\varphi_i$ denotes the position of the ith atom within this unit cell. The perturbation to the tight-binding Hamiltonian, induced by a constant bend, has the form

$$\Delta H=\sum_{\mathbf{t}}\ (\Delta\gamma_{12}^{\mathbf{t}}|\mathbf{t}\rangle_1\,{}_2\langle\mathbf{t}|+\Delta\gamma_{13}^{\mathbf{t}}|\mathbf{t}\rangle_1$$

$$\times\langle\mathbf{t}-a_1|+\Delta\gamma_{14}^{\mathbf{t}}|\mathbf{t}\rangle_1\,{}_2\langle\mathbf{t}-a_2|+\text{H. c.}), \tag{6}$$

$$\Delta\gamma_{ij}^{\mathbf{t}}=\gamma_{ij}^{(1)}\Delta\theta+\gamma_{ij}^{(2)}\Delta\theta^2,$$

where the sum runs over the unit cells within the graphene's strip, $|\mathbf{t}\rangle_1$ and $|\mathbf{t}\rangle_2$ are the atomic p_z orbitals localized on the corresponding carbon atoms 1 and 2 within the unit cell $\mathbf{t}$, and the subscipts in transfer parameters correspond to three nonequivalent pairs of carbon atoms [Fig. 1(b)]; the dependence on $\mathbf{t}$ in the right hand side of the second equation comes via the substitution of Eq. (5) into Eq. (4).

It follows from the first equation in Eq. (4) that the terms linear in $\Delta\theta$ always contain the factors $\exp(\pm i\varphi_{\mathbf{t}})$. Mapped on the graphene plane, these terms induce a periodic perturbation with the wave vector $2\pi/C_h=1/R_t$, aligned to $\mathbf{C}_h$. This coincides with the wavevector $\Delta\mathbf{k}_\perp$ spacing out the nanotube lines (Fig. 2). This means that only states belonging to nearest neighbor nanotube lines and having the same projection of the wave vector along the axis of the tube ($k_\parallel$) can be mixed by this perturbation. On the other hand, as the second of Eqs. (4) shows, some of terms proportional to $\Delta\theta^2$ will have no dependence on $\varphi_{\mathbf{t}}$ while others will contain the factors $\exp(\pm 2i\varphi_{\mathbf{t}})$. Therefore they can mix states within one nanotube line or belonging to next nearest neighbor lines, again with the same $k_\parallel$. The angular coordinates $\varphi_{\mathbf{t}}$ themselves include the dependence on the plane of bend. Indeed, it is easily seen from Fig. 1(a) that the rotation of the plane of bend of a nanotube by an angle φ_0 merely results in the change of all φ coordinates of the unit cells into $\varphi_{\mathbf{t}}+\varphi_0$.

For a primary metallic SWNT, Fig. 2 shows by open circles the states which can mix with the states from the K_1 point under an applied uniform bend. Since $\mathbf{K}_2=-\mathbf{K}_1$ the $\mathbf{k}$ states interacting with the states at the K_2 point are obtained

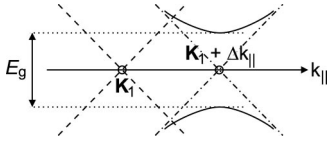

FIG. 3. The insulating gap (E_g) induced by a uniform bend in primary metallic SWNT's. Dashed lines show the dispersion of the two π bands along the nanotube line 0 (Fig. 2) in the vicinity of the K_1 point in straight nanotubes. The uniform bend leads to the shift of these bands (chain lines) and their repulsion (solid lines) opening the gap at the Fermi point.

by inverting this picture relative to the Γ point. The dispersion of the bands will therefore be equivalent in both K points, so that only the K_1 point needs to be considered. The admixture of other states leads to the interaction between two degenerate bands, $|+\mathbf{K}\rangle$ and $|-\mathbf{K}\rangle$ at the K points, described by the Hamiltonian of the following form:

$$H_K=\begin{pmatrix} A & B \\ B^* & -A \end{pmatrix}. \tag{7}$$

We are interested in the effects of the lowest order after bend's curvature. Since the terms containing $\gamma_{ij}^{(1)}$ in Eq. (4) cannot connect states with the same $\mathbf{k}$, these corrections begin with terms $\sim\Delta\theta^2$. Therefore, the only contributions to the $\Delta\theta^2$-corrections come from terms containing $\gamma_{ij}^{(2)}$ in the zeroth-order and terms containing $\gamma_{ij}^{(1)}$ in the second order via the admixture of states belonging to nearest neighbor nanotube lines (Fig. 2). Accordingly,

$$H_K=H_K^{(0)}+H_K^{(2)}, \tag{8}$$

where $H_K^{(0)}$ is just ΔH from Eq. (6) written in the basis of two degenerate states at the K point and $H_K^{(2)}$ as follows:

$$H_K^{(2)}=-\sum_\sigma\sum_l \frac{\Delta H|\sigma l\rangle\langle\sigma l|\Delta H}{\epsilon_{\sigma l}}, \tag{9}$$

where $\sigma=+$, and $-$ denotes the two π bands; $l=\pm1$ stands for nearest neighbor nanotube lines (Fig. 2), and it was taken into account that $\epsilon_{\sigma\mathbf{K}}=0$.

Equation (7) shows that the gap $2\sqrt{A^2+|B|^2}$ opens at the K point. Actually the smallest gap in the spectrum will correspond in our case to a point shifted along the line 0 in Fig. 2 by an amount of

$$\Delta k_\parallel=-A\left(\frac{\sqrt{3}}{2}V_{pp\pi}\right). \tag{10}$$

The band gap is therefore proportional to the off-diagonal matrix element between two band states in the $\mathbf{K}+\Delta\mathbf{k}_\parallel$ point (Fig. 3). Since $\Delta k_\parallel\sim\Delta\theta^2$ (via A), the difference between this matrix element and B will be of the order $\Delta\theta^4$. In the lowest order after the bend's curvature we have therefore for the bend-induced insulating gap:

$$E_g=2|B|. \tag{11}$$

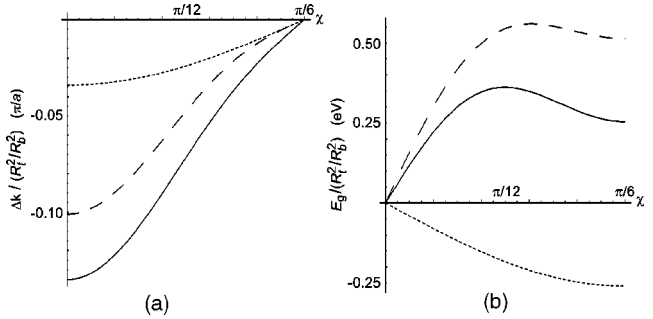

FIG. 4. The shift of the degeneracy (minimal gap) point (a) and the insulating gap (b) induced by a uniform bend in large diameter's SWNT's as a function of the chirality of the tubes. Dotted and dashed lines show the partial contributions of the zero and second order interactions, respectively (see the text for details), and the solid line shows their joint effect.

In Eqs. (10) and (11), A and B are calculated within degenerate components $|+\mathbf{K}\rangle$ and $|-\mathbf{K}\rangle$ which correspond to eigenstates in the vicinity of the K point on the line 0.

In the limit $R_t\gg r_{CC}$ [which actually works perfectly already for (10,10) tubes] the main effect of the bend comes from the change of the bond lengths, which has a simple geometrical explanation. After straightforward calculations, in this limit we obtain[21]

$$A^{(0)}=-\frac{3}{64}V'\cos 3\chi\left(\frac{R_t}{R_b}\right)^2,$$

$$A^{(2)}=\frac{3}{64}\frac{V'^2}{V_{pp\pi}}\left(\frac{5}{4}\cos 3\chi+\frac{1}{4}\cos 9\chi\right)\left(\frac{R_t}{R_b}\right)^2, \tag{12}$$

for the zeroth- and second-order contributions to the diagonal matrix element, respectively, and

$$B^{(0)}=-i\frac{3}{64}V'\sin 3\chi\left(\frac{R_t}{R_b}\right)^2,$$

$$B^{(2)}=-i\frac{3}{64}\frac{V'^2}{V_{pp\pi}}\left(\frac{5}{4}\sin 3\chi+\frac{1}{4}\sin 9\chi\right)\left(\frac{R_t}{R_b}\right)^2, \tag{13}$$

for the off-diagonal ones. In the above equations the notation $V'\equiv r_{CC}\partial V_{pp\pi}(r_{CC})/\partial r$ has been introduced. The obtained matrix elements do not depend on the origin for the φ coordinate and therefore are independent from the position of the plane of bend. Actually this dependence only arises in the two matrix elements $\langle\pm\mathbf{K}|\Delta H|\sigma l\rangle$ entering the second order contribution via exponential factors (see above), which, however, mutually cancel in Eq. (9). Note that the validity of expressions (12) and (13) does not require $R_t\ll R_b$.

Figure 4 shows the bend-induced $\Delta k_\parallel$ and E_g calculated with Eqs. (12) and (13) as function of the chiral angle for the parameters $V_{pp\pi}=-2.8$ eV and $V'=5.5$ eV.[22]. We can see that the shift of the degeneracy (minimal gap) point along the nanotube line 0 (Fig. 3) is maximal for armchair tubes, diminishes with increasing the chiral angle, and disappears in zigzag tubes. Both contributions in Eq. (12) add to each other. By contrast, the energy gap is zero in armchair tubes, then increases with chirality passing through a maximum at

some intermediate value of chiral angle, approximately in between armchair and zigzag tubes. The absence of the gap in armchair SWNT's in the lowest order after the bend's curvature was shown by Kane and Mele to be due to a pure symmetry reason.[8] The decrease of E_g for χ close to $\pi/6$ is due to a high-order harmonic term in $B^{(2)}$, which arises from the dependence of the eigenstates $|\sigma l\rangle$ in (9) on $\Delta k_\perp$. However in this case the zeroth- and second-order contributions partially cancel each other. It results from Fig. 4 that the main contribution to $\Delta k_\parallel$ and E_g arises from the second-order interaction of the states in a K point with the states from nearest neighbor nanotube lines. Although the effect of the bend rapidly diminishes with the decrease of the ratio R_t/R_b it is still sensible at realistic values of the bend's curvature. For instance, at $R_t/R_b=0.1$ the energy gap is 4 meV, which compares with the curvature-induced gap in the primary metallic SWNT of the same chirality ($\chi\approx\pi/12$) and $R_t=12$ Å.[19] However, while the latter decreases as $1/R_t^2$ the bend-induced gap increases as R_t^2 with the tube's radius, thus becoming the dominant mechanism for opening of the insulating gap starting with some value of R_t at a given bend's curvature.

It is worth mentioning that the results given by the present theory cannot be obtained within previous approaches,[8,18,19] restricted to electronic states close to K_1 and K_2 Fermi points, i.e., to states belonging only to nanotube lines which cross these points. If we would follow the same approximation we will obtain a band gap dependence on the chiral angle as one shown by the dotted line in Fig. 4(b). However, as we can see from this figure, the main contribution to the gap opening comes from the interaction of band orbitals belonging to neighbor nanotube lines [dashed line in Fig. 4(b)], which is an essential ingredient not contained in the previous treatments. This refers of course to the case $R_t \ll R_b$, when the modification of bond lengths gives the main contribution to the gap opening. When this relation does not apply the effects of orbitals misalignment and $\sigma-\pi$ hybridization (shown to be of the same order as the former effect in straight tubes[24]) become equally important and are considered elsewhere.[21]

The main difference between the effect of the local and the uniform bend on the electronic structure of long SWNT's is that the former leads to the formation of localized states without opening of the gap, while the second keeps the states delocalized over the entire length of the tube but a gap opens at the Fermi level. We envisage that direct experimental proof of the gap opening as a function of bending should become possible by tunnelling spectroscopy measurements on bent or coiled SWNT's.[16] Indeed, it was recently proven[25] that curvature-induced gaps in the meV range can be measured in straight SWNT by this technique.

Financial support from the Belgian Government (Ministerie van het Wetenschapsbeleid) and the Belgian National Science Foundation (FWO) is gratefully acknowledged.

[1] S. Iijima, Nature (London) **354**, 56 (1991)
[2] S.J. Tans, M.H. Devoret, H. Dai, A. Thess, R.E. Smalley, L.J. Georliga, and C. Dekker, Nature (London) **386**, 474 (1997).
[3] R. Saito, M. Fujita, G. Dresselhaus, and M.S. Dresselhaus, Appl. Phys. Lett. **60**, 2204 (1992).
[4] N. Hamada, S. Sawada and A. Oshiyama, Phys. Rev. Lett. **68**, 1579 (1992).
[5] J.W. Mintmire, D.H. Robertson and C.T. White, J. Phys. Chem. Solids **54**, 1835 (1993).
[6] A. Ceulemans, L.F. Chibotaru, S.A. Bovin, and P.W. Fowler, J. Chem. Phys. **112**, 4271 (2000).
[7] M.S. Dresselhaus, G. Dresselhaus, and P.C. Eklund, *Science of Fullerenes and Carbon Nanotubes* (Academic, New York, 1995).
[8] C.L. Kane and E.J. Mele, Phys. Rev. Lett. **78**, 1932 (1997).
[9] S. Iijima, C. Brabec, A. Maiti, and J. Bernholc, J. Chem. Phys. **104**, 2089 (1996).
[10] M.R. Falvo, G.J. Clary, R.M. Taylor II, V. Chi, F.P. Brooks Jr, S. Washburn, and R. Superfine, Nature (London) **389**, 582 (1997).
[11] T. Hertel, R. Martel and Ph. Avouris, J. Phys. Chem. B **102**, 910 (1998).
[12] A. Rochefort, Ph. Avouris, F. Lesage, and D.R. Salahub, Phys. Rev. B **60**, 13824 (1999).
[13] A. Rochefort, D.R. Salahub, and Ph. Avouris, Chem. Phys. Lett. **297**, 45 (1998).
[14] D. Orlikowski, H. Mehrez, J. Taylor, H. Guo, J. Wang, and C. Roland, Phys. Rev. B **63**, 155412 (2001).
[15] J. Liu, H. Dai, J.H. Hafner, D.T. Colbert, R.E. Smalley, S.J. Tans, and C. Dekker, Nature (London) **385**, 780 (1997).
[16] R. Martel, H.R. Shea, and Ph. Avouris, J. Phys. Chem. B **103**, 7551 (1999).
[17] M. Sano, A. Kamino, J. Okamura, and S. Shinkai, Science **293**, 1299 (2001).
[18] L. Yang and J. Han, Phys. Rev. Lett. **85**, 154 (2000); L. Yang, M.P. Anantram, J. Han, and J.P. Lu, Phys. Rev. B **60**, 13874 (1999).
[19] A. Kleiner and S. Eggert, Phys. Rev. B **63**, 073408 (2001).
[20] J.C. Slater and G.F. Koster, Phys. Rev. B **94**, 1498 (1954).
[21] L.F. Chibotaru, S. Compernolle, S.A. Bovin, and A. Ceulemans (unpublished).
[22] To evaluate the parameter V', following Harrison (Ref. 23) we suppose a quadratic dependence of the transfer matrix element $V_{pp\pi}$ on the interatomic distance.
[23] W.A. Harrison, *Electronic Structure and the Properties of Solids* (W. H. Freeman and Company, San Francisco, 1980).
[24] A. Kleiner and S. Eggert, Phys. Rev. B **64**, 113402 (2001).
[25] M. Ouyang, J.-L. Huang, C.L. Cheung, and C.M. Lieber, Science **292**, 702 (2001).